First Measurement of Inclusive $B \to X_s \eta$ Decays

K. Nishimura,[9] T. E. Browder,[9] I. Adachi,[10] H. Aihara,[46] K. Arinstein,[1,33] T. Aushev,[20,14] A. M. Bakich,[40] V. Balagura,[14] E. Barberio,[24] K. Belous,[13] V. Bhardwaj,[35] M. Bischofberger,[26] A. Bondar,[1,33] A. Bozek,[30] M. Bračko,[22,15] M.-C. Chang,[5] Y. Chao,[29] A. Chen,[27] K.-F. Chen,[29] P. Chen,[29] B. G. Cheon,[8] C.-C. Chiang,[29] I.-S. Cho,[50] Y. Choi,[39] J. Dalseno,[23,42] M. Danilov,[14] Z. Doležal,[2] A. Drutskoy,[4] S. Eidelman,[1,33] N. Gabyshev,[1,33] B. Golob,[21,15] H. Ha,[18] J. Haba,[10] T. Hara,[10] K. Hayasaka,[25] H. Hayashii,[26] Y. Horii,[45] Y. Hoshi,[44] W.-S. Hou,[29] H. J. Hyun,[19] T. Iijima,[25] K. Inami,[25] R. Itoh,[10] M. Iwabuchi,[50] Y. Iwasaki,[10] N. J. Joshi,[41] T. Julius,[24] J. H. Kang,[50] P. Kapusta,[30] H. Kawai,[3] T. Kawasaki,[32] H. Kichimi,[10] C. Kiesling,[23] H. J. Kim,[19] H. O. Kim,[19] M. J. Kim,[19] Y. J. Kim,[7] K. Kinoshita,[4] B. R. Ko,[18] P. Kodyš,[2] S. Korpar,[22,15] P. Križan,[21,15] T. Kumita,[47] A. Kuzmin,[1,33] Y.-J. Kwon,[50] S.-H. Kyeong,[50] J. S. Lange,[6] M. J. Lee,[38] S.-H. Lee,[18] J. Li,[9] C. Liu,[37] Y. Liu,[29] D. Liventsev,[14] R. Louvot,[20] A. Matyja,[30] S. McOnie,[40] K. Miyabayashi,[26] H. Miyata,[32] Y. Miyazaki,[25] G. B. Mohanty,[41] T. Mori,[25] E. Nakano,[34] M. Nakao,[10] H. Nakazawa,[27] Z. Natkaniec,[30] S. Nishida,[10] S. Ogawa,[43] T. Ohshima,[25] S. L. Olsen,[38,9] W. Ostrowicz,[30] G. Pakhlova,[14] C. W. Park,[39] H. Park,[19] H. K. Park,[19] K. S. Park,[39] R. Pestotnik,[15] M. Petrič,[15] L. E. Piilonen,[48] M. Röhrken,[17] S. Ryu,[38] H. Sahoo,[9] Y. Sakai,[10] O. Schneider,[20] C. Schwanda,[12] A. J. Schwartz,[4] K. Senyo,[25] O. Seon,[25] M. E. Sevior,[24] M. Shapkin,[13] C. P. Shen,[9] J.-G. Shiu,[29] F. Simon,[23,42] P. Smerkol,[15] A. Sokolov,[13] E. Solovieva,[14] M. Starič,[15] T. Sumiyoshi,[47] S. Suzuki,[36] Y. Teramoto,[34] K. Trabelsi,[10] S. Uehara,[10] T. Uglov,[14] Y. Unno,[8] S. Uno,[10] G. Varner,[9] K. E. Varvell,[40] K. Vervink,[20] C. H. Wang,[28] M.-Z. Wang,[29] P. Wang,[11] Y. Watanabe,[16] J. Wicht,[10] K. M. Williams,[48] E. Won,[18] Y. Yamashita,[31] M. Yamauchi,[10] C. C. Zhang,[11] Z. P. Zhang,[37] P. Zhou,[49] V. Zhulanov,[1,33] T. Zivko,[15] A. Zupanc,[17] and O. Zyukova[1,33]

(Belle Collaboration)

[1]*Budker Institute of Nuclear Physics, Novosibirsk*
[2]*Faculty of Mathematics and Physics, Charles University, Prague*
[3]*Chiba University, Chiba*
[4]*University of Cincinnati, Cincinnati, Ohio 45221*
[5]*Department of Physics, Fu Jen Catholic University, Taipei*
[6]*Justus-Liebig-Universität Gießen, Gießen*
[7]*The Graduate University for Advanced Studies, Hayama*
[8]*Hanyang University, Seoul*
[9]*University of Hawaii, Honolulu, Hawaii 96822*
[10]*High Energy Accelerator Research Organization (KEK), Tsukuba*
[11]*Institute of High Energy Physics, Chinese Academy of Sciences, Beijing*
[12]*Institute of High Energy Physics, Vienna*
[13]*Institute of High Energy Physics, Protvino*
[14]*Institute for Theoretical and Experimental Physics, Moscow*
[15]*J. Stefan Institute, Ljubljana*
[16]*Kanagawa University, Yokohama*
[17]*Institut für Experimentelle Kernphysik, Karlsruher Institut für Technologie, Karlsruhe*
[18]*Korea University, Seoul*
[19]*Kyungpook National University, Taegu*
[20]*École Polytechnique Fédérale de Lausanne (EPFL), Lausanne*
[21]*Faculty of Mathematics and Physics, University of Ljubljana, Ljubljana*
[22]*University of Maribor, Maribor*
[23]*Max-Planck-Institut für Physik, München*
[24]*University of Melbourne, School of Physics, Victoria 3010*
[25]*Nagoya University, Nagoya*
[26]*Nara Women's University, Nara*
[27]*National Central University, Chung-li*
[28]*National United University, Miao Li*
[29]*Department of Physics, National Taiwan University, Taipei*
[30]*H. Niewodniczanski Institute of Nuclear Physics, Krakow*
[31]*Nippon Dental University, Niigata*
[32]*Niigata University, Niigata*
[33]*Novosibirsk State University, Novosibirsk*
[34]*Osaka City University, Osaka*

[35]Panjab University, Chandigarh
[36]Saga University, Saga
[37]University of Science and Technology of China, Hefei
[38]Seoul National University, Seoul
[39]Sungkyunkwan University, Suwon
[40]School of Physics, University of Sydney, NSW 2006
[41]Tata Institute of Fundamental Research, Mumbai
[42]Excellence Cluster Universe, Technische Universität München, Garching
[43]Toho University, Funabashi
[44]Tohoku Gakuin University, Tagajo
[45]Tohoku University, Sendai
[46]Department of Physics, University of Tokyo, Tokyo
[47]Tokyo Metropolitan University, Tokyo
[48]IPNAS, Virginia Polytechnic Institute and State University, Blacksburg, Virginia 24061
[49]Wayne State University, Detroit, Michigan 48202
[50]Yonsei University, Seoul

(Received 19 August 2010; published 5 November 2010)

We report a first measurement of inclusive $B \to X_s \eta$ decays, where X_s is a charmless state with unit strangeness. The measurement is based on a pseudoinclusive reconstruction technique and uses a sample of $657 \times 10^6 B\bar{B}$ pairs accumulated with the Belle detector at the KEKB e^+e^- collider. For $M_{X_s} < 2.6\ \mathrm{GeV}/c^2$, we measure a branching fraction of $[26.1 \pm 3.0(\mathrm{stat})^{+1.9}_{-2.1}(\mathrm{syst})^{+4.0}_{-7.1}(\mathrm{model})] \times 10^{-5}$ and a direct CP asymmetry of $\mathcal{A}_{CP} = -0.13 \pm 0.04^{+0.02}_{-0.03}$. Over half of the signal occurs in the range $M_{X_s} > 1.8\ \mathrm{GeV}/c^2$.

DOI: 10.1103/PhysRevLett.105.191803 PACS numbers: 13.25.Hw, 13.30.Eg, 14.40.Nd

Decays of B mesons involving the $b \to s$ transition are an excellent tool for searches for physics beyond the standard model (SM). Theoretical treatments of these decays into exclusive hadronic final states, however, suffer from large uncertainties in the hadronization process. The uncertainties can be effectively reduced by leaving some of the final states in the calculation at the quark level, which corresponds to a measurement of an inclusive hadronic state X_s of unit strangeness.

Among such $b \to s$ decays, those involving the η and η' mesons exhibit unique properties due to interference between their underlying $SU(3)$ octet and singlet components [1]. The CLEO collaboration reported the first measurement of inclusive $B \to X_s \eta'$ with an unexpectedly large branching fraction and an X_s spectrum that peaks at high X_s mass [2], a result confirmed in improved, higher-statistics measurements [3,4]. Explanations included a large intrinsic $c\bar{c}$ component of the η' [5], the QCD anomaly mechanism [6] that couples two gluons to the flavor singlet component of the η', and also new physics sources [7]. The first is disfavored by the lack of an enhancement of $B \to \eta_c K$ relative to $B \to J/\psi K$ [8], while the second is disfavored by a measurement of $\Upsilon(1S) \to \eta' X$ [9], which indicates an $\eta' gg$ form factor that cannot explain the enhancement. A recent treatment [10] using soft collinear effective theory suggests that a measurement of the complementary process $B \to X_s \eta$ can elucidate the possible contribution from nonperturbative charm-penguin amplitudes or higher-order gluonic operators to both the η and η' processes. CLEO performed the only previous search with an upper limit of $\mathcal{B}(B \to X_s \eta) < 4.4 \times 10^{-4}$ [2].

In this Letter, we report a measurement of $B \to X_s \eta$ using a sample of $657 \times 10^6 B\bar{B}$ pairs accumulated with the Belle detector at the KEKB e^+e^- collider [11]. The Belle detector is a large solid-angle magnetic spectrometer and is described in detail elsewhere [12].

We reconstruct candidate B mesons using a pseudoinclusive method, with the X_s composed of a K^+ or $K^0_S(\to \pi^+\pi^-)$ and up to four pions, of which at most one is a $\pi^0(\to \gamma\gamma)$. This gives a total of 18 reconstructed channels and their charge-conjugates [13]. Charged pions and kaons are selected based on information from the time-of-flight, aerogel Cherenkov, and drift chamber dE/dx systems. Typical efficiencies to correctly identify kaons (pions) are above 88% (98%), with misidentification rates for pions as kaons (kaons as pions) below 12% (4%). K^0_S candidates are required to have an invariant mass within 16 MeV/c^2 (4σ) of the K^0_S mass and a displaced vertex from the interaction point. For π^0 candidates, each daughter photon is required to have energy greater than 50(100) MeV in the barrel (endcap) region and a shower shape consistent with a photon. The invariant mass of the photon pair must be within 15 MeV/c^2 (2.5σ) of the π^0 mass. The π^0 momentum is recalculated using the nominal π^0 mass. To suppress combinatorial backgrounds, we require π^0 candidates to have laboratory momenta greater than 300 MeV/c. Pions and kaons are combined to form an X_s.

Candidate η mesons are reconstructed in the $\eta \to \gamma\gamma$ mode from photons with $E_\gamma > 200$ MeV. The invariant mass of the γ-pair is required to lie between 520 MeV/c^2 and 570 MeV/c^2, or within 2σ of the nominal mass. We veto an η candidate if either of its photons

can be combined with another photon in the event to form a candidate π^0. To suppress background from radiative B decays, we require the energy asymmetry of the two photons, defined as $|E_{\gamma_1} - E_{\gamma_2}|/|E_{\gamma_1} + E_{\gamma_2}|$, to be less than 0.6. The η mass constraint [14] is used to refit the momenta of the daughter photons. To suppress secondary η mesons from $b \to c \to \eta$ chains, we retain only η candidates whose center-of-mass (cm) momentum satisfies $|\mathbf{p}^*_\eta| > 2.0$ GeV/c.

B meson candidates are formed from combinations of an X_s and an η. A beam-constrained mass, $M_{\rm bc} = \sqrt{E^2_{\rm beam}/c^4 - |\mathbf{p}^*_B|^2/c^2}$ and energy difference, $\Delta E = E_B - E_{\rm beam}$ are calculated, where $E_{\rm beam}$, $\mathbf{p}^*_B$, and E_B are the beam energy, B momentum, and B energy, all in the cm frame. The signal is obtained using fits to $M_{\rm bc}$ with $|\Delta E| < 0.1$ GeV.

We use a simulated signal Monte Carlo (MC) sample [15] consisting of $B \to K\eta$ for $M_{X_s} < 0.6$ GeV/c^2, $B \to K^*\eta$ for $M_{X_s} \in [0.8, 1.0]$ GeV/c^2, and $B \to X_s\eta$ in all other mass regions ($M_{X_s} \in [0.6, 0.8]$ GeV/c^2, and $M_{X_s} > 1.0$ GeV/c^2). For the $B \to X_s\eta$ component, fragmentation of the X_s system into hadrons is simulated by PYTHIA [16], assuming a model in which the X_s mass spectrum is flat from the $K\pi$ threshold up to 3.2 GeV/c^2. We find an average of approximately nine B candidates per event, with 10% of events having more than 20 candidates. We select the candidate with the lowest χ^2, with χ^2 defined as the sum of $\chi^2_{\Delta E} = (\Delta E/\sigma_{\Delta E})^2$, where the resolution σ_{Δ_E} is estimated separately for each reconstructed mode, and, if available, a reduced χ^2 of a vertex fit that includes all X_s daughter charged tracks except those used as part of a K^0_S candidate. The resolution in ΔE is asymmetric. It also varies by mode, with the most significant differences between modes with and without a π^0. For modes without (with) a π^0, typical ΔE resolutions are 62 (76) MeV for $\Delta E < 0$ and 29 (31) MeV for $\Delta E > 0$. After applying this procedure and applying continuum suppression cuts (described below), we select the correctly reconstructed B in 56% of simulated events.

The dominant background to $B \to X_s\eta$ comes from continuum production of quark pairs, $e^+e^- \to q\bar{q}(q = u, d, s, c)$. These events have a jetlike topology, and are suppressed relative to the spherical $B\bar{B}$ events using a Fisher discriminant [17] formed from event shape variables [18,19]. Further suppression is obtained by combining this Fisher discriminant with the cosine of the B flight direction in the cm frame and, when available, the displacement between the signal B and the other B in the event. This suppression is optimized as a function of b-flavor tag quality [20], and is approximately 34% efficient for the signal modes while suppressing over 99% of the continuum background.

Decays of the type $B \to X_c\eta$ and $B \to X_c \to X_s\eta$, where X_c is any state containing charm mesons, may have final states identical to the signal mode. We search among the candidate B decay products for combinations consistent with selected charm meson decays and veto the candidate if the mass of the reconstructed combination is within $\pm 2.5\sigma$ of the known mass. The modes and their veto widths are: $D^0 \to Kn\pi^\pm(\pi^0)$, 13.5(44.5) MeV/c^2, $D^+ \to Kn\pi^\pm(\pi^0)$, 12.5(31.3) MeV/c^2, $D^0 \to K^0_S\eta$, 31.3 MeV/c^2, $D^+_s \to \eta\pi^+$, 29.3 MeV/c^2, and $\eta_c(1S) \to \eta\pi^+\pi^-$, 85.0 MeV/$c^2$. We also veto events with an $\eta' \to \eta\pi^+\pi^-$ candidate with an invariant mass $M_{\eta\pi\pi}$ within 100 MeV/c^2 of the nominal η' mass.

Signal yields are obtained using an extended unbinned maximum likelihood fit to $M_{\rm bc}$ in 200 MeV/c^2 bins of X_s mass up to 2.6 GeV/c^2. The probability density function (PDF) for the signal is taken as a Gaussian, with the mean and width determined from the appropriate signal MC sample ($K\eta$, $K^*\eta$, or $X_s\eta$) for the mass bin. The mean and width are calibrated for small differences between the data and MC calculations using a $B \to D\pi^\pm$ control sample, with D reconstructed from a K and one to four π, with at most one π^0. All reconstructed modes are combined for the fit, and no attempt is made to separate correctly reconstructed B candidates and those with some missing or incorrectly attributed B daughters (self-cross-feed). Shapes for the charm contributions remaining after the vetoes are assigned based on a MC sample of generic $b \to c$ processes. Four separate PDFs are assigned for the largest charm backgrounds as identified in MC calculations: $B^0 \to \bar{D}^0\eta$, $B^0 \to \bar{D}^{*0}\eta$, $B^0 \to D^{(*)-}\pi^+\eta$, and $B^+ \to \bar{D}^{(*)0}\pi^+\eta$. All other $b \to c$ backgrounds are combined into another PDF. Each charm PDF consists of a Gaussian component to describe the peaking in $M_{\rm bc}$, and an empirically determined parameterization (ARGUS function) [21] to describe nonpeaking combinatorial contributions. The shape parameters are taken from the appropriate background MC sample. Normalizations of the modes $B^0 \to \bar{D}^{(*)0}\eta$ are based on the previous Belle measurement [22]. The branching fractions for the decays $B \to D^{(*)}\pi\eta$ are unknown, so their normalization is determined by a simultaneous χ^2 minimization based on the difference between the expected and observed $M_{\rm bc}$ distribution of the events in all eight veto windows. The normalization scaling of $D^-\pi^+\eta$ is assumed to be the same as of $D^{*-}\pi^+\eta$. A similar assumption is used for the $D^{(*)0}\pi\eta$ modes. The χ^2 technique is verified by repeating the optimization over the $B^0 \to \bar{D}^{(*)0}\eta$ modes, for which the results are consistent with the previous Belle measurement. This χ^2 is also used to study systematic errors on the normalizations of all charm PDFs. Normalization for the PDF that includes all other $b \to c$ modes is fixed to the MC expectation. The remaining combinatorial $q\bar{q}$ backgrounds are modeled with an ARGUS function. For the final fit, the signal yield and both the yield and shape parameter of the $q\bar{q}$ ARGUS PDF are allowed to vary.

Rare B decay backgrounds are studied with a dedicated MC sample, and include contributions from $B \to X_s\eta'$, $B \to X_s\gamma$, and $B \to X_d\eta$. These expected yields are

subtracted from the fit yield to give a final yield. The expected yields for $B \to X_s \eta'$ and $B \to X_s \gamma$ are based on the known branching fractions, and are found to be less than 0.5 events in each X_s mass bin. The $B^+ \to \pi^+ \eta$ branching fraction is also known, and the expectation is 5.2 events in the lowest bin of X_s mass. We estimate the contribution from other $B \to X_d \eta$ modes by repeating the reconstruction and the fitting procedure but replacing the K^+ candidate of X_s with a π^+ candidate. Performing these fits on data and using a dedicated $X_d \eta$ MC sample to estimate the rate to misreconstruct X_d as X_s, we estimate a total contamination of 19.1 ± 2.3 events from $X_d \eta$, distributed uniformly in the range $M_{X_s} \in [0.6, 2.6]$ GeV/c^2.

The fit to the full mass range, $M_{X_s} \in [0.4, 2.6]$ GeV/c^2, is shown in Fig. 1(a), and gives a background-subtracted yield of $1054 \pm 54^{+16}_{-18}$. We also define a high mass region, $M_{X_s} \in [1.8, 2.6]$ GeV/c^2, where the summed yield is $233 \pm 34^{+13}_{-15}$. Significances are determined in each mass bin by convolving the likelihood function with a Gaussian of width determined by the systematic errors on the yield. The maximum likelihood, $\mathcal{L}_{\max}$, and the likelihood at a signal yield of zero, $\mathcal{L}_0$, are used to determine the significance, which is defined as $\sqrt{-2\ln(\mathcal{L}_0/\mathcal{L}_{\max})}$. The significance is 23 (7) for the full (high) X_s mass range.

Reconstruction efficiencies in bins of X_s mass range from 6.5% to 0.1%, not including the branching fraction for $\eta \to \gamma\gamma$; these results are based on the signal MC calculations and assume equal production of B^+B^- and $B^0\bar{B}^0$ at $\Upsilon(4S)$. Efficiency losses are monotonic with an average of 30% efficiency loss with each increase in M_{X_s} bin. Figure 1(b) shows the differential branching fraction as a function of M_{X_s}. Table I gives the final results for each X_s mass bin. For the full M_{X_s} range, we sum the individual contributions and find the following partial branching fraction $\mathcal{B}(B \to X_s \eta; M_{X_s} \in [0.4, 2.6]\ \text{GeV}/c^2) = (26.1 \pm 3.0^{+1.9+4.0}_{-2.1-7.1}) \times 10^{-5}$, where errors are statistical, (model-independent) systematic, and decay modeling. A large fraction of the inclusive signal occurs in the high mass region, where we find $\mathcal{B}(B \to X_s \eta; M_{X_s} \in [1.8, 2.6]\ \text{GeV}/c^2) = [16.9 \pm 2.9(\text{stat})^{+1.5}_{-1.8}(\text{syst})^{+3.3}_{-5.9} \times (\text{model})] \times 10^{-5}$.

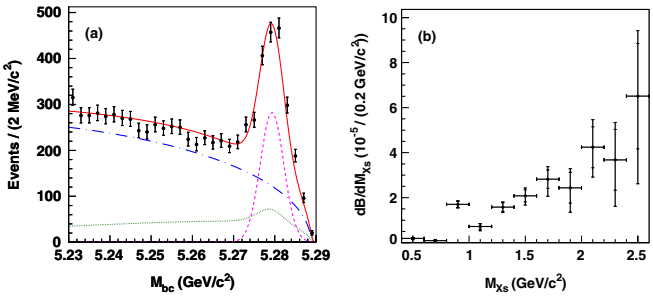

FIG. 1 (color online). (a) The $M_{\rm bc}$ distribution for the full mass range, $M_{X_s} \in [0.4, 2.6]$ GeV/c^2. The points with errors correspond to the data, while the curves correspond to the overall fit PDF (solid red), the signal PDF (dashed magenta), the sum of all $b \to c$ background PDFs (dotted green), and the combinatorial background PDF (dash-dotted blue). (b) Differential branching fraction, $d\mathcal{B}/dM_{X_s}$, for $B \to X_s \eta$. The error bars correspond to statistical error and total error. Error bars on the first two bins are smaller than the points.

The direct CP asymmetry is defined as $\mathcal{A}_{CP} = (\mathcal{B}^- - \mathcal{B}^+)/(\mathcal{B}^- + \mathcal{B}^+)$, where $\mathcal{B}^+(\mathcal{B}^-)$ is the partial branching fraction for B^+ or B^0 (B^- or $\bar{B}^0$). We measure this asymmetry in the subset of reconstructed modes in which the B flavor can be inferred from the final state (13 out of 18 modes). We adjust the fitted CP asymmetry to account

TABLE I. Measured background-subtracted signal yields (N_S), branching fractions ($\mathcal{B}$), and CP asymmetry ($\mathcal{A}_{CP}$), for each M_{X_s} range. Uncertainties on N_S are statistical. Uncertainties on $\mathcal{B}$ are statistical, systematic, and modeling, respectively. The uncertainties for $\mathcal{A}_{CP}$ are statistical and systematic.

M_{X_s} (GeV/c^2)	N_S	$\mathcal{B}(10^{-6})$	$\mathcal{A}_{CP}(10^{-2})$
0.4–0.6	60 ± 12	$1.9 \pm 0.4 \pm 0.1 \pm 0.0$	$-35 \pm 18 \pm 2$
0.6–0.8	15 ± 9	$0.9 \pm 0.5 \pm 0.1^{+0.1}_{-0.0}$	$2 \pm 40 \pm 13$
0.8–1.0	250 ± 19	$17.0 \pm 1.3 \pm 1.0 \pm 0.0$	$-4 \pm 7 \pm 2$
1.0–1.2	84 ± 14	$7.2 \pm 1.2 \pm 0.5^{+0.3}_{-1.4}$	$-26 \pm 15^{+3}_{-4}$
1.2–1.4	146 ± 17	$15.8 \pm 1.9 \pm 1.0^{+1.0}_{-1.1}$	$-22 \pm 11^{+2}_{-3}$
1.4–1.6	137 ± 18	$20.8 \pm 2.7^{+1.3+1.9}_{-1.4-2.8}$	$-15 \pm 12^{+2}_{-3}$
1.6–1.8	128 ± 18	$28.2 \pm 4.1 \pm 2.1^{+3.3}_{-6.1}$	$-25 \pm 13^{+2}_{-3}$
1.8–2.0	64 ± 18	$24.4 \pm 6.8^{+3.6+3.7}_{-3.4-7.8}$	$-31 \pm 26 \pm 6$
2.0–2.2	86 ± 18	$42.4 \pm 9.1^{+3.9+7.3}_{-4.4-8.7}$	$34 \pm 20^{+4}_{-3}$
2.2–2.4	49 ± 18	$36.8 \pm 13.5^{+5.9+7.6}_{-6.1-14.5}$	$2 \pm 32 \pm 5$
2.4–2.6	35 ± 13	$65.1 \pm 23.4^{+9.5+14.5}_{-12.9-28.3}$	$-40 \pm 36^{+7}_{-12}$
0.4–2.6	1053 ± 54	$261 \pm 30^{+19+40}_{-21-71}$	$-13 \pm 4^{+2}_{-3}$
1.0–2.6	728 ± 48	$241 \pm 30^{+18+40}_{-20-71}$	$-15 \pm 6 \pm 3$
1.8–2.6	233 ± 34	$169 \pm 29^{+15+33}_{-18-59}$	$0 \pm 14 \pm 5$

for events that are reconstructed with the wrong B flavor by multiplying the raw fitted asymmetry by a correction factor. This factor is estimated from the signal MC calculations, and ranges from unity to 1.05. The bin-by-bin results, as well as the results of separate fits for $\mathcal{A}_{CP}$ over the full X_s mass range and the range above the narrow kaonic resonances ($M_{X_s} \in [1.0, 2.6]$ GeV/c^2), are shown in Table I. For $M_{X_s} \in [0.4, 2.6]$ GeV/c^2, we find $\mathcal{A}_{CP} = -0.13 \pm 0.04^{+0.02}_{-0.03}$, with a significance of 2.6σ relative to a null asymmetry. All $\mathcal{A}_{CP}$ results that include the range $M_{X_s} \in [0.4, 0.6]$ GeV/c^2 are calculated with the assumption that the $B^+ \to \pi^+\eta$ backgrounds in this region contribute a CP asymmetry consistent with the existing measured world average [14].

Systematic errors on the fitted signal yield are dominated by PDF uncertainties. Uncertainties in the signal PDF parameters are studied using a $B \to D\pi$ control sample, while those due to normalizations and shapes for the $b \to c$ backgrounds are estimated by using comparisons between the veto window χ^2 procedure and one of the following: a repeated χ^2 procedure with relaxed assumptions, MC expectations, or, when available, previous measurements. Errors from the background subtractions are dominated by uncertainties in the estimate of backgrounds from $B \to X_d\eta$. Our estimates of these backgrounds may have included other small contributions, such as those from $B \to X_s\eta$, so we allow these estimates to vary by -100%. Positive uncertainties are estimated from the difference in expected yields assuming a flat distribution of X_d events in X_s mass versus those obtained from a MC study of cross-feed from X_d mass to X_s mass. In all cases the systematic uncertainties on the background-subtracted signal yields are at least a factor of 2 smaller than the statistical errors.

The model-independent systematic error includes contributions from the signal yield, the selection efficiency, the number of $B\bar{B}$ pairs, and the $\eta \to \gamma\gamma$ branching fraction [14]. For X_s mass bins above 1.8 GeV/c^2, the errors on the signal yields from uncertainties in the PDF shapes (primarily for the charm PDFs) dominate with a contributed relative uncertainty of 7%–18%. For the lower X_s mass bins, the efficiency error is the largest contribution with a relative uncertainty of 5%–6%. This error is the combination of individually determined contributions from control sample studies of the following: tracking, reconstruction of π^0, η, and K^0_S, particle identification, continuum suppression, and candidate selection.

We define an additional error due to modeling of the X_s system, which is studied in three parts. The first is due to the fraction of unreconstructed modes (e.g., modes with more than a total of four π's, more than one π^0, or more than one K). We vary these fractions by $\pm 30\%$ of the PYTHIA expectation and use the differences in efficiency to estimate an M_{X_s} bin-dependent uncertainty that rises with X_s mass from zero to $\pm 21.1\%$. The second is due to differences in the observed frequency of decay modes and those expected from PYTHIA. We find good agreement between data and MC calculations in the relative amounts of charged and neutral B modes, modes with K^0_S and those with K^+, and modes with one or two total π's and those with three or four total π's. However, we find a significant excess of modes without a π^0 over those with a π^0, which we attribute to inaccuracies in the PYTHIA fragmentation. To quantify this uncertainty, we reestimate the PYTHIA efficiencies with the fraction of π^0 modes adjusted to match data, and use the difference between this value and the nominal efficiency to assign an error. This error is usually only negative, due to the higher reconstruction efficiency for modes without a π^0, and is as large as -37% in the highest X_s mass bin. The final component of the modeling uncertainty is due to the assumed X_s mass spectrum. We study the efficiencies of other M_{X_s} signal MC samples where the spectrum rises toward high mass and assign errors based on the differences from the flat M_{X_s} MC calculations. Using these samples, we also study the fractions of self-cross-feed candidates that are reconstructed with an incorrect X_s mass. These effects are small compared to the first two components of the modeling error.

The systematic error on $\mathcal{A}_{CP}$ includes contributions due to: uncertainties in the PDF parameters; possible detector and measurement biases are estimated from the measured $\mathcal{A}_{CP}$ of the $B \to D\pi$ control sample and the signal MC calculations, respectively; uncertainty due to the signal model is studied by checking the fractions of events with incorrectly identified flavor using alternative M_{X_s} spectra; and possible contamination due to $B \to \pi\eta(B \to X_d\eta)$ decays is estimated by varying their A_{CP} by the measured uncertainty [14] ($\pm 100\%$).

In summary, we report the first measurement of the inclusive process $B \to X_s\eta$, and find a partial branching fraction of $\mathcal{B}(B \to X_s\eta; M_{X_s} \in [0.4, 2.6]\ \text{GeV}/c^2) = [26.1 \pm 3.0(\text{stat})^{+1.9}_{-2.1}(\text{syst})^{+4.0}_{-7.1}(\text{model})] \times 10^{-5}$. The measured M_{X_s} dependent branching fractions are consistent with the known $B \to K\eta$ and $B \to K^*(892)\eta$ processes [23]. In the high mass region, $M_{X_s} \in [1.8, 2.6]$ GeV/c^2, which is above any significant contributions from previously measured exclusive processes [24], we observe a signal with a 7σ significance. We also measure the CP asymmetry of $B \to X_s\eta$, both as a function of M_{X_s} and for the full mass range, where we find $\mathcal{A}_{CP} = -0.13 \pm 0.04^{+0.02}_{-0.03}$, consistent with rough theoretical expectations [10]. No theoretical prediction is currently available for the shape of the M_{X_s} spectrum. However, the similarity in spectral shape to $B \to X_s\eta'$ and the lack of strong suppression of the $B \to X_s\eta$ branching fraction relative to the η' mode imply that the origin of the large contribution in the η' mode is also common to the η mode [10], and disfavors η' specific mechanisms [5,6].

We thank the KEKB group for excellent operation of the accelerator, the KEK cryogenics group for efficient solenoid operations, and the KEK computer group and the NII for valuable computing and SINET3 network

support. We acknowledge support from MEXT, JSPS and Nagoya's TLPRC (Japan); ARC and DIISR (Australia); NSFC (China); MSMT (Czechia); DST (India); MEST, NRF, NSDC of KISTI (Korea); MNiSW (Poland); MES and RFAAE (Russia); ARRS (Slovenia); SNSF (Switzerland); NSC and MOE (Taiwan); and DOE (USA).

[1] H. J. Lipkin, Phys. Lett. B **254**, 247 (1991).
[2] T. E. Browder *et al.* (CLEO Collaboration), Phys. Rev. Lett. **81**, 1786 (1998).
[3] G. Bonvicini *et al.* (CLEO Collaboration), Phys. Rev. D **68**, 011101 (2003).
[4] B. Aubert *et al.* (BaBar Collaboration), Phys. Rev. Lett. **93**, 061801 (2004).
[5] I. E. Halperin and A. Zhitnitsky, Phys. Rev. Lett. **80**, 438 (1998).
[6] D. Atwood and A. Soni, Phys. Lett. B **405**, 150 (1997).
[7] W. S. Hou and B. Tseng, Phys. Rev. Lett. **80**, 434 (1998).
[8] K. W. Edwards *et al.* (CLEO Collaboration), Phys. Rev. Lett. **86**, 30 (2001).
[9] M. Artuso *et al.* (CLEO Collaboration), Phys. Rev. D **67**, 052003 (2003).
[10] J. Chay, C. Kim, A. K. Leibovich, and J. Zupan, Phys. Rev. D **76**, 094031 (2007).
[11] S. Kurokawa and E. Kikutani, Nucl. Instrum. Methods Phys. Res., Sect. A **499**, 1 (2003).
[12] A. Abashian *et al.* (Belle Collaboration), Nucl. Instrum. Methods Phys. Res., Sect. A **479**, 117 (2002).
[13] Throughout this Letter, the inclusion of the charge-conjugate mode decay is implied unless otherwise stated.
[14] C. Amsler *et al.* (Particle Data Group), Phys. Lett. B **667**, 1 (2008).
[15] We use the EvtGen *B* meson decay generator, D. J. Lange, Nucl. Instrum. Methods Phys. Res., Sect. A **462**, 152 (2001). The detector response is simulated with GEANT; R. Brun *et al.*, GEANT 3.21 CERN Report No. DD/EE/84-1, 1984.
[16] T. Sjostrand, S. Mrenna, and P. Skands, J. High Energy Phys. 05 (2006) 026.
[17] R. O. Duda, P. E. Hart, and D. G. Stork, *Pattern Classification* (John Wiley & Sons, New York, 2001), 2nd ed..
[18] G. C. Fox and S. Wolfram, Phys. Rev. Lett. **41**, 1581 (1978).
[19] S. H. Lee *et al.* (Belle Collaboration), Phys. Rev. Lett. **91**, 261801 (2003).
[20] H. Kakuno *et al.*, Nucl. Instrum. Methods Phys. Res., Sect. A **533**, 516 (2004).
[21] H. Albrecht *et al.* (ARGUS Collaboration), Phys. Lett. B **241**, 278 (1990).
[22] S. Blyth *et al.* (Belle Collaboration), Phys. Rev. D **74**, 092002 (2006).
[23] S. J. Richichi *et al.* (CLEO Collaboration), Phys. Rev. Lett. **85**, 520 (2000).
[24] B. Aubert *et al.* (BaBar Collaboration), Phys. Rev. Lett. **97**, 201802 (2006).